Microbial Pathogenesis 218 (2026) 108668

Contents lists available at ScienceDirect

Microbial Pathogenesis

journal homepage: www.elsevier.com/locate/micpath

Transcriptional profiling of the *Crocodylus porosus* liver cell response to Kunjin virus reveal novel insights into the host-virus interface

Suchandan Sikder [a], Manoharan Kumar [a], Matt Field [a], Peter Mee [b], Alex Loukas [a], Karla J. Helbig [c], Subir Sarker [c,d,*]

[a] Australian Institute of Tropical Health and Medicine, James Cook University, Cairns, QLD, 4878, Australia
[b] Agriculture Victoria Research, AgriBio Centre for AgriBioscience, Bundoora, VIC, 3083, Australia
[c] Department of Microbiology, Anatomy, Physiology & Pharmacology, La Trobe University, Bundoora, VIC, 3083, Australia
[d] Biomedical Sciences & Molecular Biology, College of Medicine and Dentistry, James Cook University, Townsville, QLD, 4814, Australia

ARTICLE INFO

Keywords:
Kunjin2011 virus
LV-1 cell
Infection kinetics
RNAseq
CXCL10

ABSTRACT

Crocodilians possess a unique and robust immune system, offering a valuable model for studying vertebrate antiviral responses and informing zoonotic disease surveillance and therapeutic discovery. Building on our previous work that characterized crocodilian immune responses to synthetic viral mimics, this study investigates the innate immune dynamics of *Crocodylus porosus* liver (LV-1) cells infected with the Kunjin2011 virus, a genetically and antigenically related member of the West Nile virus (WNV) complex. A time-course infection assay was conducted up to 192 h post-infection (hpi), combining viral infectivity analysis with transcriptomic profiling. Delayed Kunjin2011 viral replication was confirmed via qRT-PCR, revealing a clear exponential phase after 48 hpi and peaking at 192 hpi. RNA sequencing demonstrated progressive transcriptional reprogramming in LV-1 cells, with early gene expression changes modest but becoming pronounced by 192 hpi. Differential expression analysis identified 1428 upregulated and 1308 downregulated genes, with temporal shifts from early activation to late-stage suppression. Principal component analysis and hierarchical clustering further supported a time-dependent divergence in host transcriptional responses. Notably, CXCL10, a key immune-associated chemokine, exhibited a biphasic expression pattern, with an early peak at 8 hpi, suppression at intermediate time points, and renewed induction from 72 hpi onwards. Together, these results demonstrate that Kunjin2011 infection elicits a dynamic and time-dependent transcriptional response in *C. porosus* liver cells, characterized by early activation of innate immune pathways followed by extensive transcriptional remodeling during prolonged infection. This study provides new insights into crocodilian host responses to flavivirus infection and establishes a foundation for future investigations of antiviral immunity and host–virus interactions in reptiles.

1. Introduction

The innate immune response to viral infections in reptiles, particularly crocodilians, remains poorly understood [1–3]. As ancient ectothermic vertebrates, crocodiles exhibit a distinctive immune architecture that may harbor unique antiviral defense mechanisms [4,5]. Investigating these responses is essential for advancing our understanding of host-pathogen co-evolution, clarifying the ecological role of reptiles in virus transmission, and uncovering pathways of cross-species viral spread [6,7]. Additionally, these studies may uncover ancestral immune strategies that have been altered or lost in mammals, amphibians, reptile and birds, offering valuable insights for comparative immunology and potential applications in biomedical research [8,9].

The innate immune response serves as the first line of defense against viral infections, acting rapidly to detect and limit viral replication [10]. This response is mediated by a network of pattern recognition receptors (PRRs), including Toll-like receptors (TLRs), RIG-I-like receptors (RLRs), and NOD-like receptors (NLRs), which recognize conserved pathogen-associated molecular patterns (PAMPs) such as viral RNA and DNA [11]. Upon recognition, these receptors initiate intracellular signaling cascades that lead to the production of type I interferons (IFNs) and proinflammatory cytokines, establishing an antiviral state and coordinating the activation of the adaptive immune system. This early response is critical for limiting viral spread, reducing disease severity,

* Corresponding author.Biomedical Sciences & Molecular Biology, College of Medicine and Dentistry, James Cook University, Townsville, QLD, 4814, Australia.
E-mail address: subir.sarker@jcu.edu.au (S. Sarker).

https://doi.org/10.1016/j.micpath.2026.108668
Received 26 January 2026; Received in revised form 27 June 2026; Accepted 28 June 2026
Available online 29 June 2026

and shaping long-term immunity. In birds, the innate immune system shares several conserved features with mammals but also includes distinct elements, such as a truncated interferon system and species-specific PRRs [12,13].

In our previous work, we demonstrated that primary crocodile liver cells respond dynamically to RNA and DNA viral mimic stimulations [14]. This included upregulation of key antiviral genes such as viperin, Mx1, IRF7, IRF1, RIG-I, IFN-α, and IFN-ω, along with many uncharacterized transcripts, suggesting that crocodiles may utilize mammalian-like TLR and cytosolic RNA-sensing pathways.

Building on these findings, the present study investigates the transcriptional response of LV-1 cell line to infection with Kunjin2011 virus, a subtype of West Nile virus and a member of the *Flaviviridae* family known to cause neurological disease in humans and animals. Beyond its relevance as an arbovirus of medical importance, Kunjin virus also poses a major threat to the crocodile farming industry, where it has been associated with skin lesions that reduce leather quality and cause substantial economic losses [15]. Recent research, including vaccine trials, highlights both the urgency of this issue and the potential for translational solutions to protect the multi-million-dollar crocodile farming sector [16]. Despite its relevance, the interaction between Kunjin virus and reptilian hosts has not been explored in detail. We infected LV-1 cells and harvested samples at multiple time points to study both early and late-phase immune responses using high-throughput RNA sequencing. This study aims to reveal new insights into the host-virus interface in reptiles, addressing a significant gap in our understanding of flavivirus-host interactions across vertebrate lineages while also informing strategies for disease mitigation in crocodile aquaculture.

2. Materials and methods

2.1. Cells and Kunjin2011 quantification

The Kunjin2011 virus used in this study was propagated in C6/36 cell line derived from *Aedes albopictus* (Asian tiger mosquito) [17]. A viral plaque assay was performed to determine the titer of Kunjin2011 virus, expressed as plaque-forming units per milliliter (PFU/mL). Briefly, Vero cells were cultured in Dulbecco modified minimum essential medium (DMEM; Life Technologies) supplemented with 10% fetal bovine serum (FBS) and maintained at 37°C in a 5% CO_2 atmosphere. Kunjin2011 virus samples were serially diluted in 10 folds from a neat preparation with a TCID50 10^7 and added to the Vero cell monolayers in petri dishes to allow viral absorption and infection. Infections were assessed at Days 1, 2, 3, 4, 5, and 6 post-infections. Plates were incubated at 37°C to permit viral replication and cell-to-cell spread. After 6 days, cells were fixed and stained with crystal violet, enabling visualization of plaques—clear zones where infected cells were lysed—against a background of stained, viable cells. Each plaque corresponded to a single infectious virus particle. The viral titer was calculated as 1.88×10^9 PFU/mL, using the formula: PFU/mL = (No. of plaques × Dilution factor)/Volume of inoculum (mL).

2.2. LV-1 cell culture and stimulation with Kunjin2011 virus

The LV-1 used in this study was originally established by the Berrimah Veterinary Laboratory (Department of Primary Industry and Resources, Government of the Northern Territory, Australia). Cells were maintained at 28°C in the absence of CO_2, using M199 medium supplemented with 10% fetal calf serum (FCS) and antibiotics, as described previously [18]. The protocol for viral stimulation was adapted from established methods [18], with slight modifications to optimize infection conditions for this cell line. For viral challenge, LV-1 cells were seeded [2×10^5 cells/T-75 flask] and subsequently stimulated with Kunjin2011 virus at a final concentration of 5×10^5 PFU/mL. Uninfected cells were included as controls. Each treatment group included three biological replicates. Cells were harvested at multiple time points such as 8-, 24-, 48-, 72-, 96-, and 192-h post-infection (hpi) to capture the infection kinetics and temporal dynamics of host gene expression in response to viral stimulation. This time-course design enabled detailed investigation of the progression and modulation of innate immune responses following exposure to the virus.

2.3. Fluorescent focus assay

To further assess the kinetics of Kunjin2011 virus infection in LV-1 cells, a fluorescent focus assay (FFA) was performed. At 8, 24, 48, 72, 96, and 192 h post-infection (hpi), cells were washed twice with phosphate-buffered saline (PBS, Sigma-Aldrich). Following removal of the culture supernatant, cell monolayers were fixed by addition of 100 μL per well of ice-cold acetone:methanol (1:1, v/v) and incubated at 4°C for 15 min. The fixative was removed, and cells were rehydrated with 100 μL PBS prior to immunostaining. After removal of PBS, Kunjin2011 viral antigens were detected by incubation with 40 μL per well of anti-dengue capsid primary antibody (Abcam, UK) diluted in PBS containing 1% (w/v) bovine serum albumin (BSA) for 1 h at room temperature. Cells were then washed with PBS (100 μL per well) and incubated with a fluorophore-conjugated secondary antibody diluted in PBS containing 1% BSA (40 μL per well) for 1 h at 4°C in the dark. Following incubation, cells were washed twice with PBS (100 μL per well) to remove unbound antibody. Infected cells were visualized by fluorescence microscopy, and fluorescent foci, defined as discrete clusters of infected cells, were counted. Fluorescent images were acquired using a fluorescence microscope equipped with DAPI and FITC filter sets at 20× magnification. Viral infection was detected as green fluorescence (FITC-positive cells), while cell nuclei were counterstained with DAPI and visualized as blue fluorescence.

2.4. RNA isolation, quality assessment, and RT-PCR

Total cellular RNA was extracted from each biological replicate using the Isolate II RNA Mini Kit (Bioline), which included an on-column DNase I digestion step to eliminate genomic DNA contamination. RNA concentration and purity were assessed using a NanoDrop spectrophotometer, while RNA integrity was evaluated with the Agilent 2100 Bioanalyzer (Agilent Technologies, USA). Only RNA samples with A260/280 ratios ≥1.8 and RNA Integrity Numbers (RIN) ≥ 9.0 were deemed suitable for downstream applications, ensuring high-quality input material across all time points of the viral stimulation time course. First-strand complementary DNA (cDNA) synthesis was carried out using reverse transcription reactions, followed by quantitative real-time PCR (qPCR) using an ABI 7000 sequence detection system. Primer sequences and qPCR cycling conditions were adopted from previously established protocols [18]. GAPDH was used as the reference (housekeeping) gene for normalization of gene expression in LV-1 cells. Gene-specific primers were used to assess the expression of viperin (as described previously) and CXCL10. The primer sequences for CXCL10 were forward 5′-TGTGAGCGCCTTGAGATCAT and reverse 5′-GCTGCCACGTTTAGACTTGTT. This methodology enabled accurate quantification of gene expression levels in response to Kunjin2011 virus stimulation, facilitating the analysis of antiviral and immune-related transcriptional responses in the LV-1 cell line.

2.5. Construction and sequencing of strand-specific RNA-seq libraries

Strand-specific RNA-seq libraries were prepared using the Illumina TruSeq® RNA Sample Preparation v2 Kit with modifications [14]. A total of fifteen libraries were constructed: three biological replicates each for control and *Kunjin2011 virus*-stimulated samples at four time points (8 h, 48 h, 96 h, and 192 h), using 0.5 μg of total RNA per sample. Total RNA was denatured at 65°C for 5 min to remove secondary structures and improve poly(A) + RNA binding to oligo-dT beads. Polyadenylated RNA was then isolated according to the manufacturer's

protocol. Fragmentation and priming of mRNA were performed using 19.5 μL of the Elute, Prime, and Fragment Mix containing random hexamers at 94°C for 8 min.

First-strand cDNA synthesis was conducted using SuperScript® II reverse transcriptase (Invitrogen™) and Illumina's First Strand Master Mix at 25°C for 10 min, 42°C for 50 min, and 70°C for 15 min. Second-strand synthesis followed immediately by adding 25 μL of Second Strand Master Mix and incubating at 16°C for 1 h. The resulting double-stranded cDNA was purified using AMPure XP beads (Invitrogen™). Blunt-end repair was carried out in a 100 μL reaction with diluted End Repair Control and End Repair Mix, followed by incubation at 30°C for 30 min. After purification, a single "A" nucleotide was added to the 3′ ends of the blunt-ended cDNA in a 30 μL reaction, incubated at 37°C for 30 min and 70°C for 5 min. Adaptor ligation was performed with indexed Illumina® adaptors in a 37.5 μL reaction, incubated at 30°C for 10 min, and stopped with 5 μL of Stop Ligation Buffer. The adaptor-ligated cDNA was again purified using AMPure XP beads.

PCR amplification of the libraries was carried out in 50 μL reactions containing adaptor-ligated DNA, PCR Primer Cocktail, and PCR Master Mix. Thermal cycling was performed as follows: 98°C for 30 s; 15 cycles of 98°C for 10 s, 60°C for 30 s, and 72°C for 30 s; with a final extension at 72°C for 5 min. PCR products were purified to remove adaptor dimers using AMPure XP beads and eluted in 30 μL of resuspension buffer. Library quality and insert size (100–125 bp) were assessed using an Agilent TapeStation at the Australian Genome Research Facility (AGRF, Melbourne). Libraries were normalized, pooled equimolarly, and sequenced on the Illumina® HiSeq platform using paired-end chemistry.

2.6. Functional analysis of differentially expressed genes (DEGs)

Raw 100 bp single-red reads quality checked using FastQC. Later, raw reads with adapter and low quality scores were trimmed using BBDuk module from BBTools package (version 39.06) (https://jgi.doe.gov/data-and-tools/software-tools/bbtools/) [19]. Final clean reads were quality checked using FastQC (https://www.bioinformatics.babraham.ac.uk/projects/fastqc/). Clean reads were mapped using STAR (version 2.7.1a) tool against the Australian saltwater crocodile (*Crocodylus porosus*) reference genome version CroPor_comp1 (GTF annotation version: CroPor_comp1.113) from Ensemble database. STAR [20] output bam files were used to calculate gene wise read counts and low gene counts were filtered using the default option in ConsensusDE [21] in R version 4.4.2, Bioconductor version. Furthermore, using ConsensusDE (RUV option) we removed Unwanted variants or Batch effect. EDASeq (version 2.36.0) was used to perform normalization on 12,537 filtered genes out of 19,207 total genes. Later, the PCA plot and differential gene expression were generated using ConsensusDE (version 1.24.0) package. Differential expression results from the intersection of three DE tools DESeq2 [22] edgeR v4 [23], and limma [24] used to obtain DEs. We filtered significant genes using two cutoffs: log2-fold change (LFC) from −1 to 1 were excluded and an intersect P value < 0.05 was considered. Common genes from control vs various time point were compared and plotted as top 10 GO terms and KEGG enrichment plots using ggplot2 [25] and clusterProfiler R package [26].

3. Results

The immune response to viral infections in crocodiles is of considerable interest, as it offers valuable insights into evolutionary immunology, antiviral drug discovery, wildlife conservation, and zoonotic disease surveillance [27]. Owing to their unique and robust immune systems, crocodilians serve as important models for both basic and translational biomedical research [2,28–30].

In our earlier study, we investigated the response of the LV-1 to synthetic DNA and RNA viral mimics [14]. Building on that work, the current project aimed to characterize the innate immune response of *C. porosus* to Kunjin2011 virus, a member of the West Nile virus (WNV) complex, which is genetically and antigenically similar to WNV. A time-course infection study was conducted using the LV-1 cell line, with sampling at 8 h, 24 h, 48 h, 96 h, and 192 h post-infection to monitor immune activation. In parallel, a comprehensive genomic analysis of *C. porosus* was performed to identify key genes involved in antiviral immunity.

3.1. Kinetics of Kunjin2011 in LV-1 cells

We aimed at characterizing the infection kinetics of the Kunjin2011 (KunNSW2011) virus in LV-1 cells, the *C. porosus* liver cell line (LV-1) was inoculated with the virus and maintained at 28°C in M199 medium supplemented with 10% fetal calf serum and antibiotics, under atmospheric conditions (no CO_2). Observable signs of infection did not appear until after 24 h. By 48 h post-infection, green fluorescence indicative of viral infection became apparent and continued to intensify progressively, reaching a peak by the endpoint at 192 h (Fig. 1). In contrast, uninfected control cells showed no green fluorescence. Analysis of viral replication revealed a 48-h lag phase, followed by a marked exponential increase in viral activity over the remaining duration of the 192-h observation period.

3.2. Dynamic gene expression changes in LV-1 cell in response to Kunjin2011 virus infection

To investigate the temporal gene expression profiles and their involvement in immune responses, RNA sequencing (RNA-seq) was performed on crocodile LV-1 cells infected with the Kunjin2011 virus at 8-, 48-, 96-, and 192-h post-stimulation (hps) (Figs. 2 and 3). Clean RNA-seq reads aligned uniquely to the *C. porosus* reference genome, with uniform coverage across gene bodies, indicating no bias from random priming or subsequent processing. Principal Component Analysis (PCA) showed that samples from control and 8h, 48h and 96h groups clustered more closely than those from the 192h group (Fig. 2A), suggesting modest gene expression changes up to 96h and pronounced changes by 192h.

Differential expression (DE) analysis identified a total of 1428 significantly upregulated and 1308 significantly downregulated genes in virus-infected cells compared to controls (Fig. 2B). At 8h, the number of upregulated genes exceeded downregulated ones, but this trend reversed by 48h. At 96h, the number of upregulated genes again surpass the number of downregulated genes and remained consistent till 192h. Only 67 genes remained consistently upregulated, and just 9 were consistently downregulated throughout the time course (Tables 1 and 2). These results suggest that prolonged Kunjin2011 infection leads to a progressive downregulation of gene expression in LV-1 cells.

To visualize gene expression changes across all time points, volcano plots were generated for each group (Fig. 2C), showing strong correlations between fold change and statistical significance. Pairwise comparisons between time points (e.g., 8h vs. 48h/96h/192h, 48h vs. 96h/192h, and 96h vs. 192h) were also performed (Fig. 3), have revealing clear clustering patterns and distinct gene expression profiles that differentiate each stimulated group of *C. porosus* LV-1 cells.

3.3. Enriched KEGG pathways in LV-1 cells in response to Kunjin2011 virus infection

Top 20 over-represented KEGG pathway enrichment analysis revealed several significantly enriched pathways (Fig. 4). Results showed that LV-1 cells rapidly upregulated genes involved in cytokine–cytokine receptor interactions, as well as TLR, C-type lectin (Clec), RIG-I–like, and NOD-like receptor signaling pathways, along with activation of cell adhesion molecules, within 8 h of viral infection. Between 48- and 96-h post-infection, relatively few immune response genes were differentially expressed. However, by 192 h post-infection, there was an upregulation of apoptotic genes, suggesting that prolonged infection

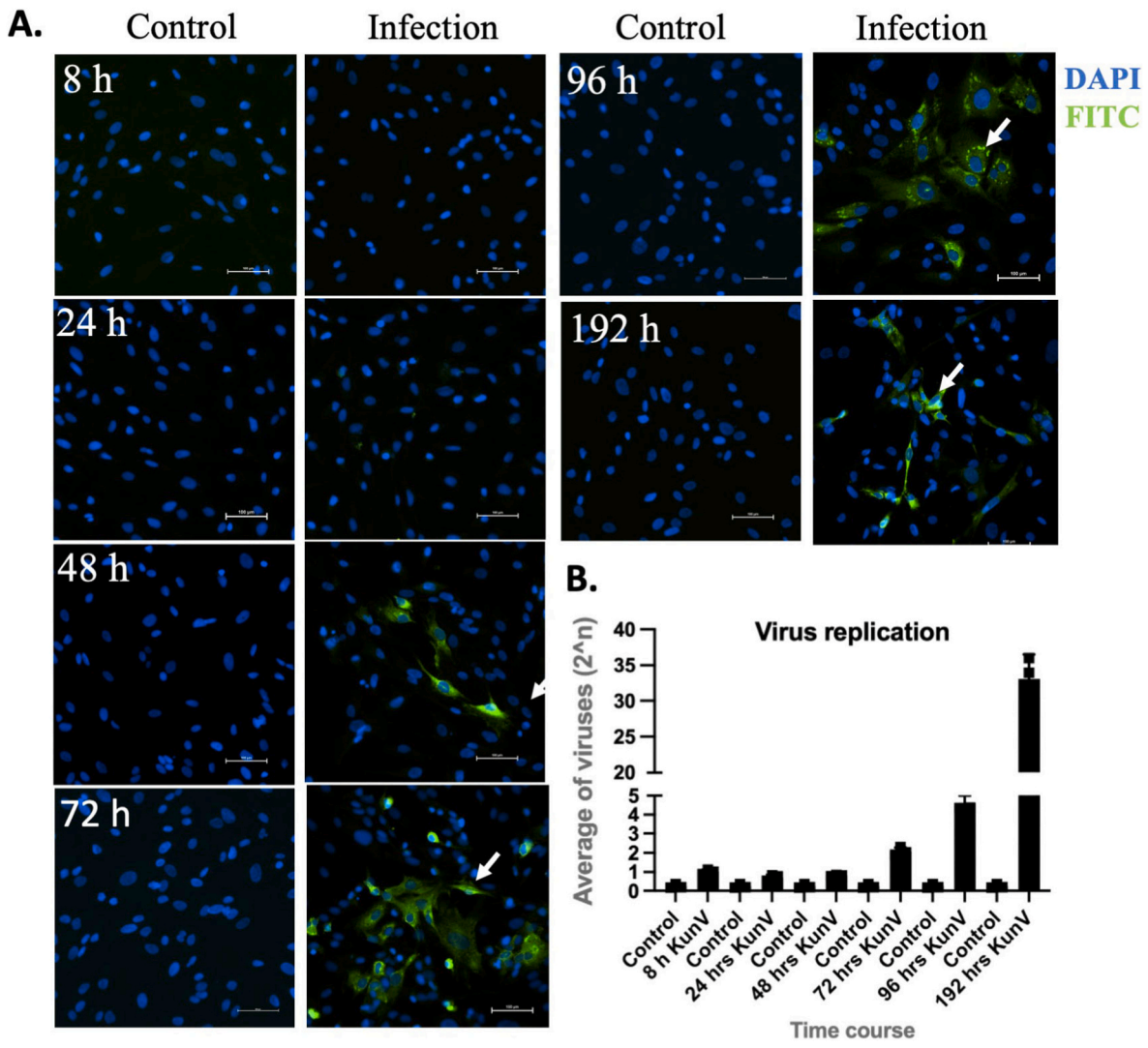

Fig. 1. Infection kinetics of Kunjin2011 (KunNSW2011) virus in LV-1 cells. The LV-1 cells were infected with the Kunjin2011 virus [2×10^5 cells/T-75 flask and 5×10^5 FFU/mL] and incubated at 28°C in M199 medium supplemented with 10% FCS and antibiotics, without CO_2. (A) Viral infection became evident after 48 h and progressively increased until the experimental endpoint at 192 h. Uninfected control cells appeared morphologically normal. Infected cells were visualized using a fluorescence microscopy at 20× magnification, with infection indicated by FITC fluorescence (green, marked by arrows). (B) Viral replication showed an exponential increase throughout the 192-h time course.

induced stress responses. leading to cell death.

3.4. Gene Ontology biological process terms enriched in LV1 cells following infection

Gene Ontology (GO) biological process analysis showed that early infection (8 h) led to the upregulation of genes associated with immune responses, including cellular responses to lipopolysaccharide and cell migration (Fig. 5). As the infection progressed from 48 to 192 h, many genes involved in DNA regulation, signal transduction, DNA repair and damage response, and cell adhesion were downregulated. These findings suggest that after the initial infection response, LV-1 cells attempt to restore homeostasis by balancing gene expression to return to an infection-free state.

3.5. Post RNAseq validation of CXCL-10 expression in LV-1 cells following Kunjin2011 virus infection

We selected CXCL10 for quantitative real-time PCR validation because it showed the strongest and most biologically relevant induction among the antiviral and inflammatory genes identified, and it is a well-established marker of interferon-mediated viral response, making it an appropriate representative target to confirm the RNA-seq findings [14]. CXCL10 expression exhibited a rapid and transient induction, peaking at 8 h post-infection, followed by a marked decline at 24 h and remaining low until 72 h (Fig. 6). After this point, its expression increased exponentially, indicating a biphasic response. In contrast, the expression of the control gene, viperin, showed a steady and gradual increase from 8 to 192 h post-infection. Notably, by 192 h, the expression levels of CXCL10 and viperin converged, reaching comparable levels, suggesting coordinated regulation of these genes at the later stage of infection. These findings highlight distinct temporal dynamics of antiviral gene expression, reflecting their potentially different roles during early and late phases of host immune response.

4. Discussion

This study provides the first comprehensive analysis of the innate immune response of *Crocodylus porosus* liver cells (LV-1) to Kunjin2011 virus, a member of the *West Nile virus* (WNV) complex. By integrating infection kinetics, transcriptomic profiling, and gene-specific validation, we delineate a dynamic antiviral response that highlights both

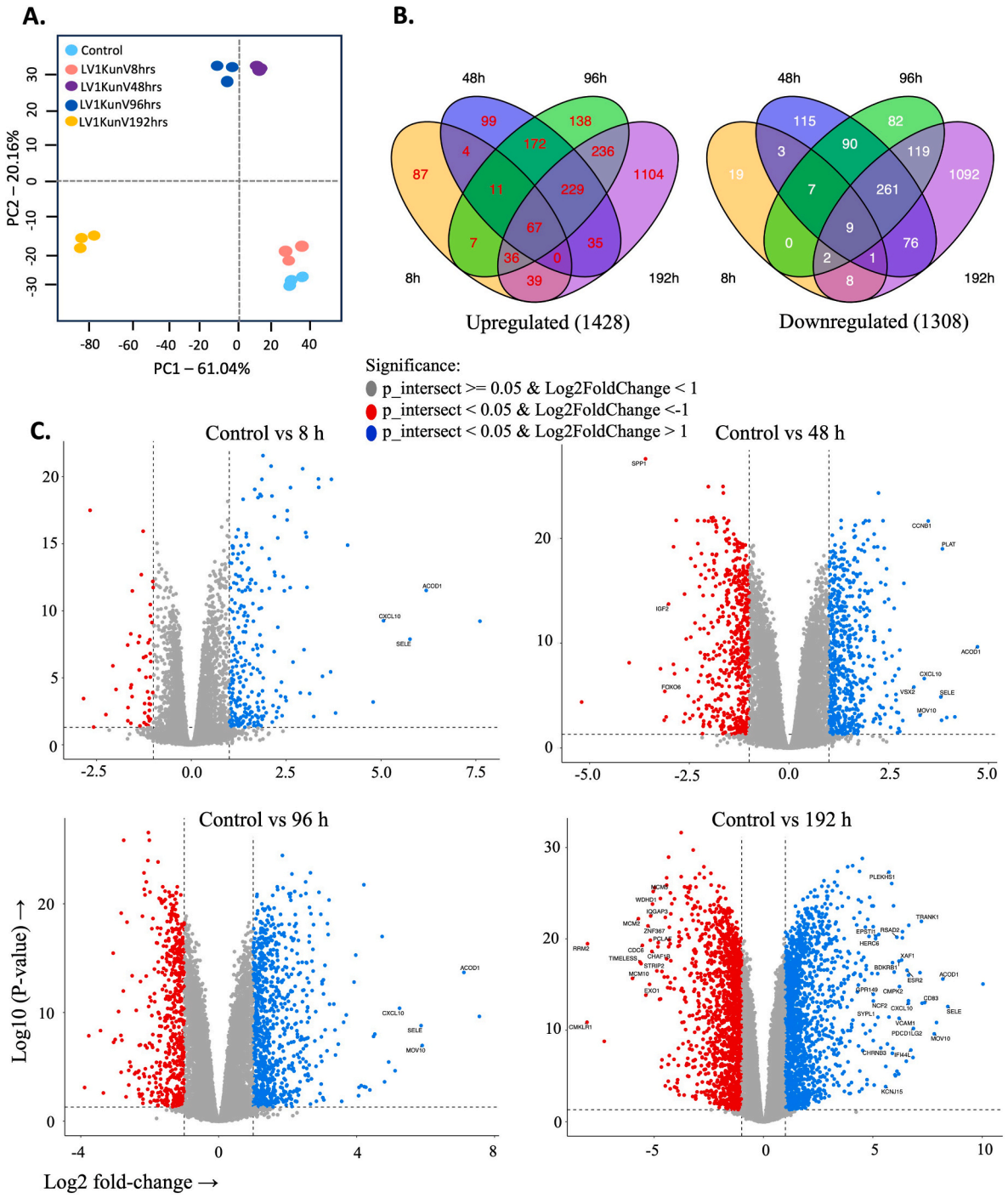

Fig. 2. Transcriptomic profiling of LV-1 cells following time-course stimulation with Kunjin virus. (A) Principal component analysis (PCA) reveals distinct clustering of gene expression patterns at various time points post-infection. (B) Venn diagram showing unique and shared upregulated and downregulated genes between control and Kunjin2011-infected LV-1 cells across time points. (C) Volcano plots illustrating differentially expressed genes in Kunjin2011-infected LV-1 cells. The x-axis represents gene enriched in Control < - log2(FC) - > Enriched in LV1KunV 8 h, 48 h, 96 h and 192 h. Significantly regulated genes are highlighted.

conserved and potentially unique features of crocodilian immunity.

Our infectivity assays confirmed that Kunjin2011 efficiently infects and replicates in c6/36 insect and LV-1 cells, with a delayed onset of detectable infection followed by a progressive increase in viral replication over a six-day period. This prolonged replication window, coupled with the absence of early cytopathic effects, suggests a tolerant or delayed lytic response, contrasting with many mammalian systems where flavivirus infection typically elicits rapid cytopathic effects [31, 32]. The prolonged infection kinetics observed in this study are likely influenced by the incubation temperature of 28°C, which, although lower than the 37°C commonly used in mammalian flavivirus studies, is essential for maintaining the physiological relevance of the crocodilian LV-1 cell line. In mammalian cells, flavivirus replication often peaks within 48–72 h [33], whereas Kunjin2011 replication in LV-1 cells peaked at 192 hpi. Lower temperatures can slow cellular metabolism, viral replication, and antiviral signaling, contributing to delayed infection dynamics. These findings highlight the importance of considering host temperature physiology when comparing flavivirus–host interactions across vertebrate species. These findings also raise intriguing questions about the mechanisms by which crocodilian cells regulate

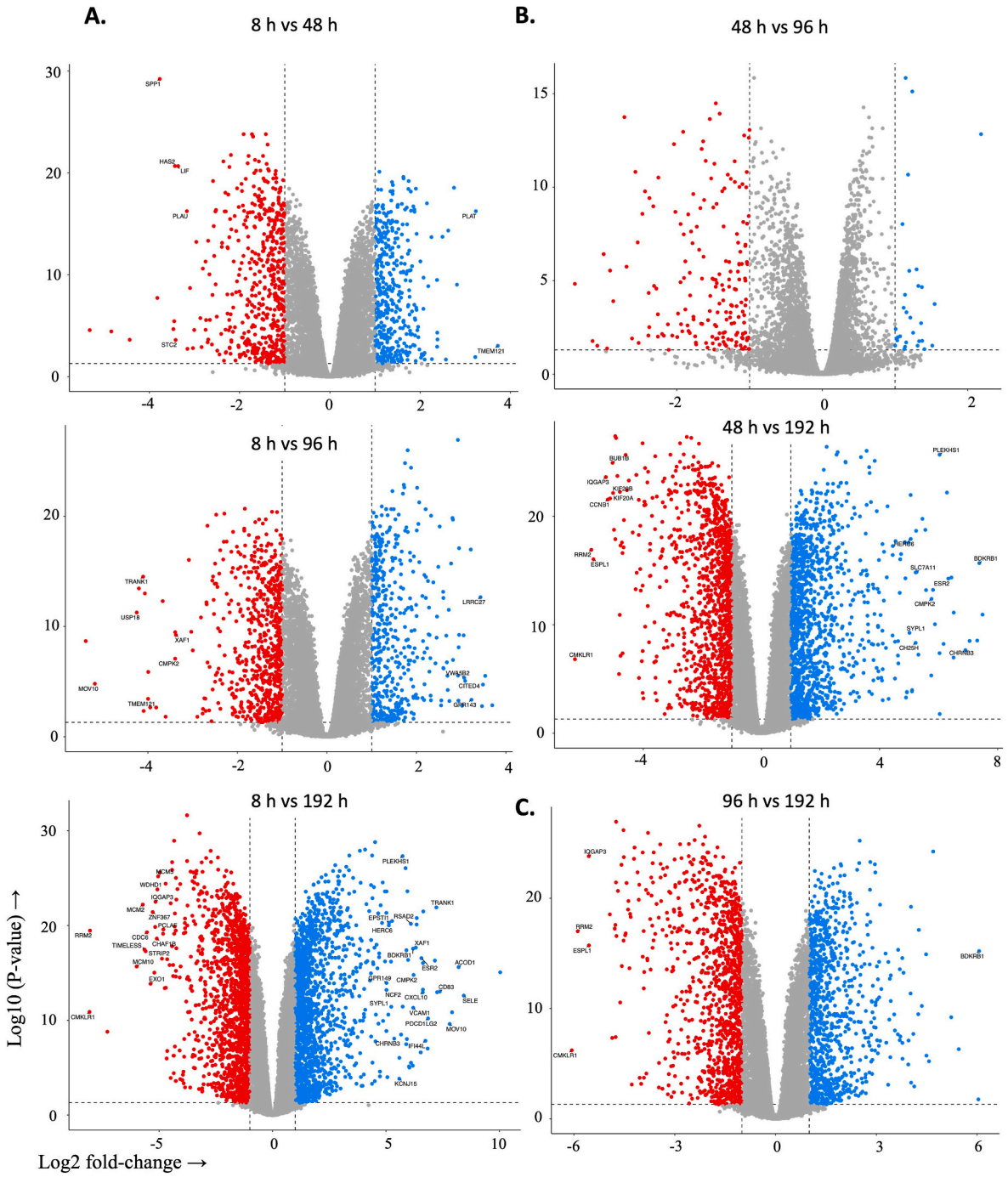

Fig. 3. Comparative analysis of RNA sequencing data from time-course stimulation of LV-1 cells with Kunjin virus. (A) Volcano plots showing differentially expressed genes (DEGs) between 8 h and later time points (48 h, 96 h, and 192 h) in Kunjin2011-infected LV-1 cells. (B) Comparison of DEGs between 48 h and 96 h/192 h post-infection. (C) DEG analysis comparing 96 h to 192 h post-infection. Significantly regulated genes are highlighted.

viral replication and maintain cellular integrity during prolonged infection.

Although direct comparisons were not performed in this study with birds and mammals, the infection kinetics observed in LV-1 cells differ from those commonly reported in mammalian flavivirus models, where viral replication is often accompanied by more rapid cytopathic effects and earlier peak viral titers [34]. In contrast, Kunjin2011-infected LV-1 cells supported prolonged viral replication with limited evidence of early cellular damage. Similar patterns of infection tolerance have been reported in several ectothermic vertebrates [14,35], where lower metabolic rates and distinct immune strategies may permit extended host–virus coexistence. This observation raises the possibility that crocodilian cells may employ mechanisms that balance viral containment with preservation of cellular integrity during infection. However, comparative studies involving reptilian, avian, and mammalian systems will be required to determine whether these responses represent lineage-specific adaptations or conserved vertebrate antiviral strategies.

Transcriptomic analyses revealed robust transcriptional changes in response to viral infection, particularly at the late stage (192 h post-infection). Principal component analysis and hierarchical clustering indicated that while early time points (8 h, 48 h) showed relatively modest changes in gene expression, a substantial shift occurred after

Table 1
The consistently upregulated genes for Kunjin virus stimulated versus control LV-1 cells at 8 h, 96 h and 192 h post stimulation. Unavailable gene name and description were not shown.

Gene ID	Gene name	Gene description	LogFC	Interest P values
ENSCPRG00005015793	TNFAIP2	TNF alpha induced protein 2	4.07754963	9.72E-29
ENSCPRG00005005375	DHX58	DExH-box helicase 58 [Source:UniProtKB	4.3414497	5.40E-25
ENSCPRG00005001541	TNFAIP3	TNF alpha induced protein 3	4.76543731	7.33E-23
ENSCPRG00005004540	BCO2	Beta-carotene oxygenase 2	4.65692456	5.21E-22
ENSCPRG00005008433	RSAD2	Radical S-adenosyl methionine domain containing 2	6.09914781	6.58E-21
ENSCPRG00005018750	CYP26B1	Cytochrome P450 family 26 subfamily B member 1	2.4549151	1.86E-21
ENSCPRG00005016034	RAB38	RAB38, member RAS onco family	2.96724726	3.19E-21
ENSCPRG00005009375	IRF1	Interferon regulatory factor 1	3.00647727	9.79E-21
ENSCPRG00005000694	APOBEC1	Apolipoprotein B mRNA editing enzyme catalytic subunit 1	4.58401371	1.05E-18
ENSCPRG00005001083	HIVEP2	HIVEP zinc finger 2	2.81088149	1.22E-19
ENSCPRG00005002148	TMEM100	Transmembrane protein 100	3.1200239	3.69E-18
ENSCPRG00005018657	ACOD1	Aconitate decarboxylase 1	8.20154819	2.43E-16
ENSCPRG00005000077	G0S2	G0/G1 switch 2	4.33663906	1.12E-15
ENSCPRG00005006846	CXCL10	C-X-C motif chemokine ligand 10	6.62298581	1.14E-13
ENSCPRG00005006820	UBALD2	UBA like domain containing 2	1.57402537	5.65E-16
ENSCPRG00005011191	PRR5L	Proline rich 5 like	1.32640654	1.20E-15
ENSCPRG00005007044	GPR149	G protein-coupled receptor 149	5.02235053	1.15E-14
ENSCPRG00005011334	PLEKHG5	Pleckstrin homology and RhoGEF domain containing G5	1.36508088	8.52E-15
ENSCPRG00005013931	NCF2	Neutrophil cytosolic factor 2	5.02198714	6.25E-14
ENSCPRG00005008996	KLHL24	Kelch like family member 24	2.81409488	1.19E-13
ENSCPRG00005005030	SELE	Selectin E	8.42981983	2.51E-13
ENSCPRG00005002774	CD83	CD83 molecule	7.37367837	9.21E-14
ENSCPRG00005014472	VCAM1	Vascular cell adhesion molecule 1	6.20063743	4.81E-12
ENSCPRG00005006907	ZNF469	Zinc finger protein 469	1.76505692	2.05E-11
ENSCPRG00005011440	CHGB	Chromogranin B	1.4895539	2.60E-11
ENSCPRG00005011065	OPTC	Opticin	3.06305928	1.24E-10
ENSCPRG00005004350	PDCD1LG2	Programmed cell death 1 ligand 2	6.85612648	6.34E-11
ENSCPRG00005009438	ADAMTS10	ADAM metallopeptidase with thrombospondin type 1 motif 10	3.54059234	7.11E-10
ENSCPRG00005012252	IRGQ	Immunity related GTPase Q	2.3863487	1.77E-08
ENSCPRG00005005088	POMGNT2	Protein O-linked mannose N-acetylglucosaminyltransferase 2 (beta 1,4-)	1.85020657	2.84E-08
ENSCPRG00005001192	SPON2	Spondin 2	1.88103312	2.50E-07
ENSCPRG00005000173	DHRS3	Dehydrogenase/reductase 3	1.27168196	1.69E-07
ENSCPRG00005016184	RGS20	Regulator of G protein signaling 20	2.44883899	2.82E-07
ENSCPRG00005010681	SLC18A2	Solute carrier family 18 member A2	2.21101919	1.36E-06
ENSCPRG00005016038	PCP4	Purkinje cell protein 4	3.00597748	2.20E-06
ENSCPRG00005016194	UMODL1	Uromodulin like 1	1.57586358	4.29E-06
ENSCPRG00005012195	TBXA2R	Thromboxane A2 receptor	2.00088067	2.60E-05
ENSCPRG00005003462	HBZ	Hemoglobin subunit zeta	2.38467079	0.000588569
ENSCPRG00005011071	FMOD	Fibromodulin	1.88832341	0.00471428
ENSCPRG00005004925	FMO3	Flavin containing dimethylaniline monoxygenase 3	2.0561032	0.003783005

Table 2
The consistently downregulated genes for Kunjin virus stimulated versus control LV-1 cells at 8 h, 96 h and 192 h post stimulation. Unavailable gene name and description were removed from the table.

Gene ID	Gene name	Gene description	LogFC	Interest P values
ENSCPRG00005017402	SLC6A9	Solute carrier family 6 member 9	−1.9833603	4.27E-18
ENSCPRG00005005100	MTCL3	MTCL family member 3	−2.6858575	9.49E-17
ENSCPRG00005008465	TMED6	Transmembrane p24 trafficking protein 6	−2.0122893	1.18E-07
ENSCPRG00005015977	FAM221A	Family with sequence similarity 221 member A	−1.662101	1.21E-05
ENSCPRG00005015607	DAO	D-amino acid oxidase	−1.0684049	0.000466535

96 h, reflecting an evolving immune response. Strikingly, a progressive downregulation of gene expression was observed as infection progressed to 48 h, with more than 1300 genes significantly downregulated by 192 h. This broad transcriptional suppression may reflect host antiviral strategies, virus-mediated immune evasion, or cellular stress responses, underscoring the complexity of host-pathogen interactions in crocodilian cells [10,14].

Only 67 genes were consistently upregulated throughout the infection, and nine were persistently downregulated, highlighting the highly dynamic and context-specific nature of gene regulation during flavivirus infection in crocodilian cells. This plasticity likely reflects an evolutionary balance between antiviral defense and maintaining cellular homeostasis, an adaptation possibly shaped by the reptiles' long evolutionary history and environmental exposure to diverse pathogens. In this study, the majority of genes upregulated following Kunjin virus infection were associated with pro-inflammatory and antiviral responses. These included TNF-α–induced proteins, which contribute to antiviral signaling [36]; neutrophil cytosolic factor, a key component of the NADPH oxidase complex responsible for generating reactive oxygen species for pathogen clearance [37]; vascular cell adhesion molecule-1 (VCAM-1), which mediates leukocyte adhesion and transendothelial migration [38]; and ADAMTS10, a metalloprotease essential for extracellular matrix organization and remodeling [39] (Table 1). This pattern differs from the transcriptional profile observed following dsRNA stimulation of LV1 cells [14], where C-X-C chemokine motifs predominated. Notably, programmed cell death 1 ligand 2 (PD-L2) was consistently upregulated in both Kunjin virus infection and dsRNA stimulation. In contrast, most downregulated genes in our dataset were linked to metabolic or catalytic processes, such as Transmembrane p24 trafficking protein 6, involved in ER–Golgi trafficking, and D-amino acid oxidase, which mediates oxidative deamination of D-amino acids.

Kunjin virus infection of LV1 cells shows a clear, stage-specific

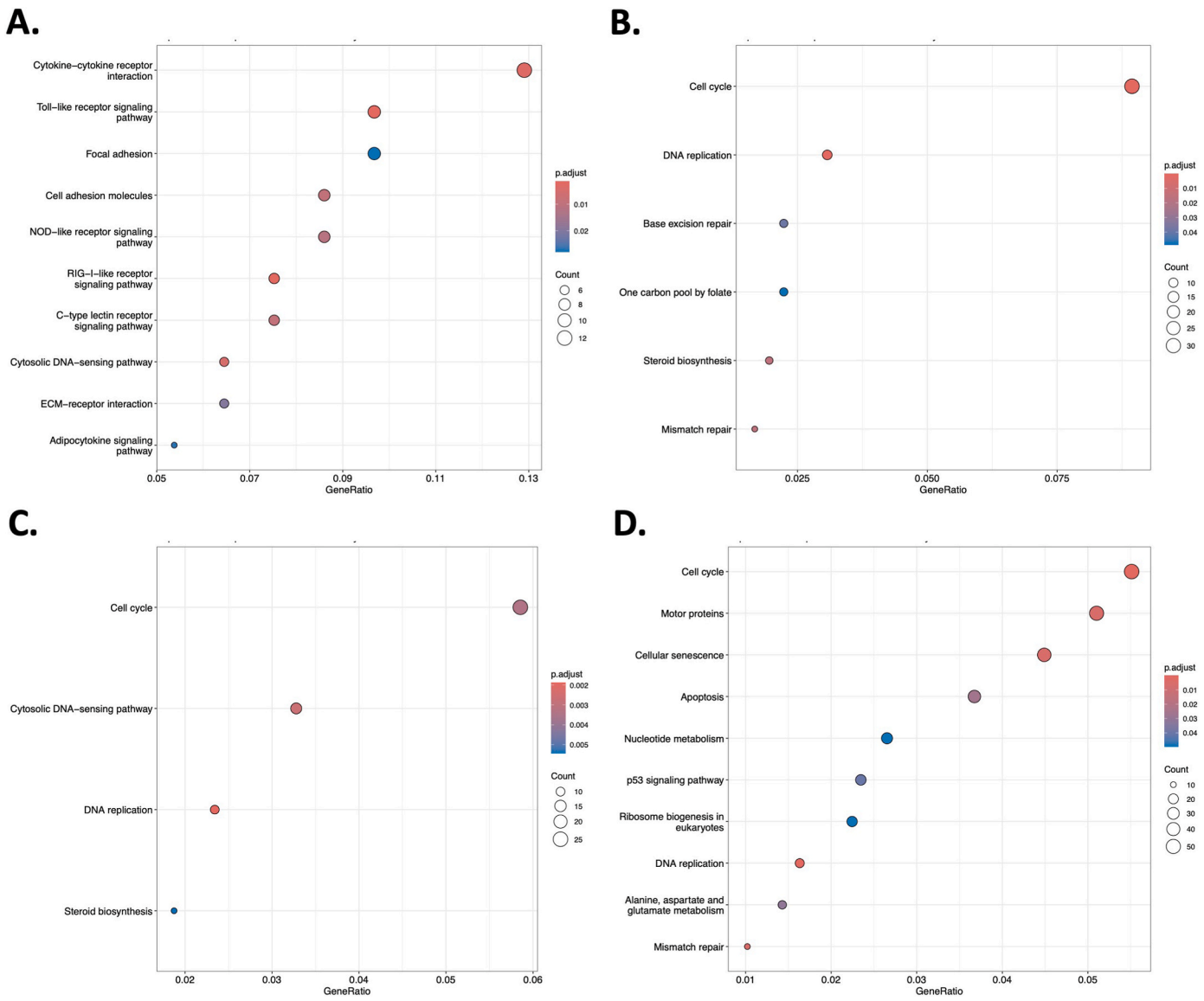

Fig. 4. Top 20 enriched KEGG pathways in LV1 cells following Kunjin virus infection at 8, 48, 96, and 192 h. KEGG pathway analysis of DEGs identified the top 20 enriched pathways in LV1 cells at 8 h (A), 48 h (B), 96 h (C), and 192 h (D) post-infection.

progression of host responses. At 8 hpi, cells mounted a strong innate immune reaction marked by activation of multiple pattern-recognition receptor families, including the unexpected engagement of cytosolic DNA-sensing pathways, alongside early disruption of extracellular matrix and adhesion signaling. By 48–96 hpi, this response transitions toward metabolic reprogramming and genome-maintenance activities, with coordinated induction of one-carbon metabolism, nucleotide synthesis, DNA repair pathways, and steroid/sterol biosynthesis, suggesting a host attempt to support both viral replication and cellular survival.

By 192 hpi, the transcriptomic profile shifts again, showing combined features of replication stress, cell-cycle dysregulation, p53 activation, senescence and apoptosis, together with paradoxical increases in ribosome biogenesis and cytoskeletal/motor-protein pathways. These late changes indicate escalating genotoxic stress and translational collapse characteristic of a chronic or terminal infection state. Although a substantial population of LV-1 cells remained attached and detectable at 192 hpi, as demonstrated by DAPI staining and fluorescence microscopy, we cannot exclude the possibility that prolonged culture and persistent infection contributed to cellular stress, senescence, or apoptosis-related transcriptional changes. Therefore, the late-stage transcriptomic profile likely reflects a combination of virus-specific responses and the physiological consequences of long-term infection. Consistent with this possibility, prolonged Kunjin2011 infection was associated with substantial downregulation of host transcripts together with enrichment of KEGG pathways related to cell-cycle disruption, DNA replication, and mismatch repair. Alternatively, the enrichment of p53 signaling, cellular senescence, and apoptosis pathways suggests that the observed transcriptional decline may also represent a host response to prolonged infection and accumulated cellular stress. The simultaneous activation of these pathways indicates that by 192 hpi, LV-1 cells have likely transitioned from an active antiviral state toward a stressed or terminal cellular state, which may contribute to the widespread changes in gene expression observed at this late stage of infection.

Complementary Gene Ontology analysis further supported these findings, highlighting that early infection enhances the expression of genes involved in immune responses, such as those mediating responses to lipopolysaccharide and promoting cell migration. However, with continued infection from 48 to 192 h, a downregulation of genes related to DNA regulation, signal transduction, DNA repair, damage response, and cell adhesion was evident. This shift may represent an attempt by LV-1 cells to restore homeostasis and limit cellular damage after the acute immune activation phase [40,41]. These results suggest a dynamic

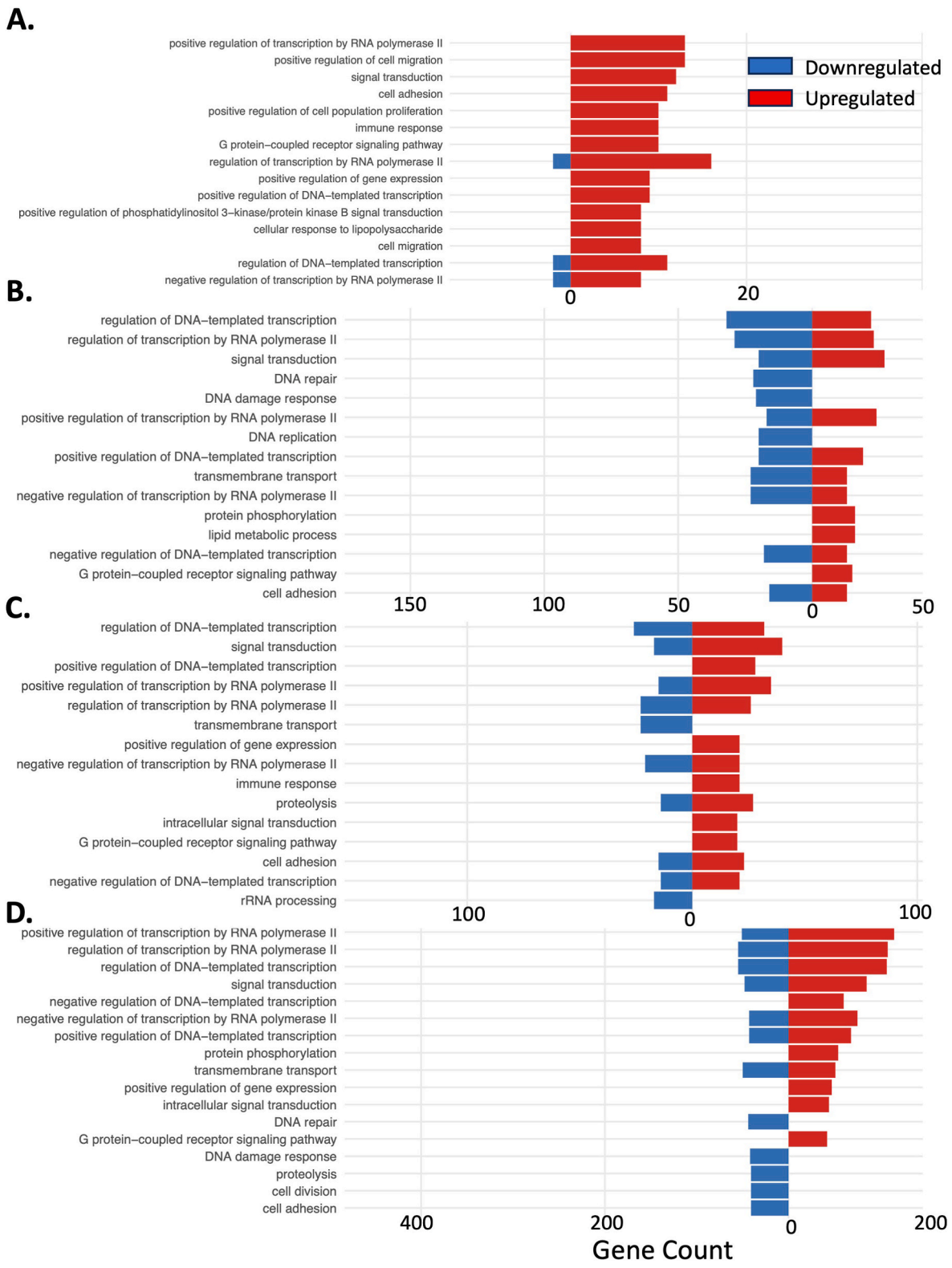

Fig. 5. Gene Ontology biological process terms in LV1 cells following Kunjin virus infection. GO analysis of biological process terms in LV1 cells at 8 h (A), 48 h (B), 96 h (C), and 192 h (D) post-infection.

interplay between an early, potent immune activation and a later effort to re-establish cellular equilibrium, with persistent infection ultimately leading to apoptosis and potential loss of cell viability.

Our RNA-seq analysis identified several key antiviral and inflammatory mediators—including TNFα-induced protein, interferon regulatory factors (IRFs), and CXCL10—that were markedly upregulated in Kunjin virus–infected LV1 cells. We selected CXCL10 for RT-PCR validation because it exhibited the most robust and biologically meaningful induction among these genes, and its well-established role as an interferon-responsive chemokine makes it an ideal representative marker to confirm our RNA-seq findings [14]. The biphasic expression profile of CXCL10, a chemokine central to leukocyte recruitment and

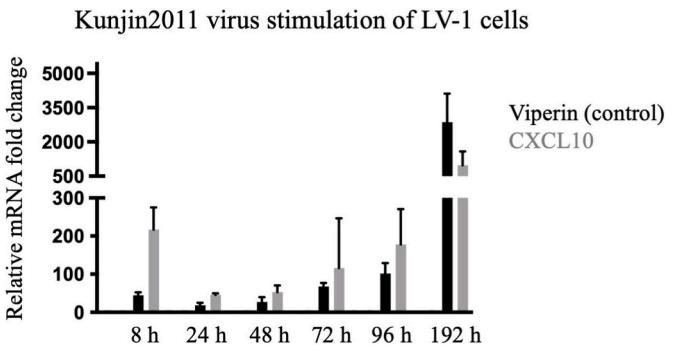

Fig. 6. Quantitative real-time PCR analysis of selected candidate gene expression following Kunjin2011 virus infection. Viperin expression was initially lower than that of CXCL10 but reached comparable levels by 192 h post-infection.

antiviral defense [42,43], further underscores the temporal complexity of the crocodilian immune response. The transient suppression of CXCL10 expression between 24 and 72 hpi may reflect several non-mutually exclusive mechanisms. One possibility is that Kunjin2011 actively modulates interferon-dependent signaling pathways during the early stages of replication to evade host antiviral responses, a strategy reported for several flaviviruses [44,45]. Alternatively, the reduction in CXCL10 expression may represent a host regulatory mechanism designed to limit excessive inflammation and potential immunopathology following the initial antiviral response [42]. Although the present study cannot distinguish between these possibilities, the subsequent re-induction of CXCL10 at later time points suggests that increasing viral burden eventually overcomes this period of suppression, leading to renewed activation of antiviral signaling pathways. In contrast, viperin—a classical interferon-stimulated gene (ISG)—showed sustained upregulation, indicating a more continuous antiviral function. The convergence of expression levels for both genes by 192 hpi suggests a coordinated late-phase antiviral response aimed at restricting viral dissemination while preventing excessive inflammation.

In short, the temporal transcriptional patterns observed in this study may reflect a dynamic balance between host defense mechanisms and viral persistence strategies. The rapid activation of innate immune pathways during the early stages of infection is likely advantageous to the host [10], enabling prompt recognition of viral RNA and induction of antiviral mediators aimed at restricting viral replication. However, the subsequent broad suppression of gene expression and the delayed peak in viral replication suggest that Kunjin2011 may partially evade or modulate host immune responses, creating a cellular environment that supports continued viral propagation. From the host perspective, the transition toward apoptosis, senescence, and stress-response pathways at later stages of infection may represent a protective mechanism to limit viral spread by eliminating infected cells [46]. Conversely, excessive activation of these pathways could contribute to tissue damage and loss of cellular function. The biphasic expression of CXCL10 further suggests a tightly regulated immune response, in which early inflammatory signaling is subsequently dampened and later reactivated as viral burden increases. Together, these findings highlight the complex interplay between antiviral defense, immune regulation, and viral adaptation during Kunjin2011 infection of crocodilian cells.

As a limitation, we were unable to validate other strongly upregulated genes such as TNFα-induced protein and IRFs, which may also contribute significantly to Kunjin virus–host interactions. Furthermore, the stability of GAPDH expression was not independently validated across all infection time points; therefore, we cannot exclude the possibility that virus-induced metabolic changes may have influenced its suitability as a reference gene. Future studies will incorporate broader qRT-PCR panels and functional assays to confirm the expression patterns of these additional genes and elucidate their roles in orchestrating the antiviral and inflammatory responses in LV1 cells.

5. Conclusion

Our findings highlight *C. porosus* as a valuable non-model system for studying vertebrate antiviral immunity. The data presented here not only enhance our understanding of crocodilian immune responses but also offer broader insights into the evolutionary diversity of antiviral strategies among vertebrates. Future studies leveraging in vivo models, primary immune cells, and comparative analyses with birds and mammals could further elucidate the mechanisms underpinning these responses and identify conserved versus lineage-specific elements of flavivirus immunity. These results may also inform translational research, including the identification of novel antiviral targets or pathways that are functionally conserved across species. Furthermore, understanding the crocodilian response to zoonotic viruses such as *West Nile virus* may have implications for wildlife disease surveillance and the assessment of reptiles' role in virus transmission dynamics.

Funding

Subir Sarker is the recipient of an Australian Research Council Discovery Early Career Researcher Award (grant number DE200100367) funded by the Australian Government. The funders had no role in the design of the study; in the collection, analyses, or interpretation of data; in the writing of the manuscript, or in the decision to publish the results. The authors also like to thank La Trobe University for the financial support under Start Up Grant to SS.

CRediT authorship contribution statement

Suchandan Sikder: Formal analysis, Methodology, Validation, Visualization, Writing – original draft, Writing – review & editing. **Manoharan Kumar:** Formal analysis, Methodology, Validation, Visualization, Writing – review & editing. **Matt Field:** Validation, Visualization, Writing – review & editing. **Peter Mee:** Methodology, Writing – review & editing. **Alex Loukas:** Validation, Writing – review & editing. **Karla J. Helbig:** Conceptualization, Supervision, Writing – review & editing. **Subir Sarker:** Conceptualization, Data curation, Formal analysis, Funding acquisition, Investigation, Methodology, Project administration, Resources, Software, Supervision, Validation, Visualization, Writing – original draft, Writing – review & editing.

Declaration of competing interest

The authors declare that they have no known competing financial interests or personal relationships that could have appeared to influence the work reported in this paper.

Acknowledgments

The authors would like to thank the Berrimah Veterinary Laboratory (Department of Primary Industry and Resources, Government of Northern Territory, Australia) for providing the *C. porosus* liver cell line (LV-1) used in this experiment.

Data availability

The study sequences are available in the National Center for Biotechnology Information (NCBI) under BioProject accession number PRJNA1403063. The raw Illumina sequence read data generated in this study have been deposited at the NCBI sequence read archive [SRA (https://www.ncbi.nlm.nih.gov/sra)] under accession numbers SRR36840913-SRR36840927.

References

[1] E.K. Field, A. Hartzheim, J. Terry, G. Dawson, N. Haydt, L.A. Neuman-Lee, Reptilian innate immunology and ecoimmunology: what do we know and where are we going? Integr. Comp. Biol. 62 (2022) 1557–1571.

[2] A. Tankrathok, B. Mahong, S. Roytrakul, S. Daduang, Y. Temsiripong, S. Klaynongsruang, N. Jangpromma, Proteomic analysis of crocodile white blood cells reveals insights into the mechanism of the innate immune system, Heliyon 10 (2024) e24583.

[3] L.M. Zimmerman, The reptilian perspective on vertebrate immunity: 10 years of progress, J. Exp. Biol. 223 (2020).

[4] R.S. Seymour, C.L. Bennett-Stamper, S.D. Johnston, D.R. Carrier, G.C. Grigg, Evidence for endothermic ancestors of crocodiles at the stem of archosaur evolution, Physiol. Biochem. Zool. 77 (2004) 1051–1067.

[5] S.A. Williams, F.T. Lay, G.K. Bindra, S. Banjara, I.K.H. Poon, T.K. Phan, M. Kvansakul, M.D. Hulett, Crocodile defensin (CpoBD13) antifungal activity via pH-dependent phospholipid targeting and membrane disruption, Nat. Commun. 14 (2023) 1170.

[6] A.G. Bean, M.L. Baker, C.R. Stewart, C. Cowled, C. Deffrasnes, L.F. Wang, J. W. Lowenthal, Studying immunity to zoonotic diseases in the natural host - keeping it real, Nat. Rev. Immunol. 13 (2013) 851–861.

[7] M. Vinkler, S.R. Fiddaman, M. Těšický, E.A. O'Connor, A.E. Savage, T.L. Lenz, A. L. Smith, J. Kaufman, D.I. Bolnick, C.S. Davies, N. Dedić, A.S. Flies, M.M. G. Samblás, A.E. Henschen, K. Novák, G. Palomar, N. Raven, K. Samaké, J. Slade, N.K. Veetil, E. Voukali, J. Höglund, D.S. Richardson, H. Westerdahl, Understanding the evolution of immune genes in jawed vertebrates, J. Evol. Biol. 36 (2023) 847–873.

[8] K. Buchmann, Evolution of innate immunity: clues from invertebrates via fish to mammals, Front. Immunol. 5 (2014) 459.

[9] M. Riera Romo, D. Pérez-Martínez, C. Castillo Ferrer, Innate immunity in vertebrates: an overview, Immunology 148 (2016) 125–139.

[10] S.R. Paludan, T. Pradeu, A. Pichlmair, K.B. Wray, J.G. Mikkelsen, D. Olagnier, T. H. Mogensen, Early host defense against virus infections, Cell Rep. 43 (2024) 115070.

[11] D. Li, M. Wu, Pattern recognition receptors in health and diseases, Signal Transduct. Targeted Ther. 6 (2021) 291.

[12] S.N. Neerukonda, U. Katneni, Avian pattern recognition receptor sensing and signaling, Vet. Sci. 7 (2020).

[13] N.C. Smith, M.L. Rise, S.L. Christian, A comparison of the innate and adaptive immune systems in cartilaginous fish, ray-finned fish, and lobe-finned fish, Front. Immunol. 10 (2019) 2292.

[14] S. Sarker, Y. Wang, B. Warren-Smith, K.J. Helbig, Dynamic changes in host gene expression following in vitro viral mimic stimulation in crocodile cells, Front. Immunol. 8 (2017) 1634.

[15] S.R. Isberg, J.L. Moran, R. De Araujo, N. Elliott, S.S. Davis, L. Melville, First evidence of Kunjin strain of West Nile virus associated with saltwater crocodile (Crocodylus porosus) skin lesions, Aust. Vet. J. 97 (2019) 390–393.

[16] G. Habarugira, J.J. Harrison, J. Moran, W.W. Suen, A.M.G. Colmant, J. Hobson-Peters, S.R. Isberg, H. Bielefeldt-Ohmann, R.A. Hall, A chimeric vaccine protects farmed saltwater crocodiles from West Nile virus-induced skin lesions, npj Vaccines 8 (2023) 93.

[17] R.A. Mann, M. Fegan, K. O'Riley, J. Motha, S. Warner, Molecular characterization and phylogenetic analysis of murray valley encephalitis virus and West Nile virus (Kunjin subtype) from an arbovirus disease outbreak in horses in Victoria, Australia, in 2011, J. Vet. Diagn. Invest. 25 (2013) 35–44.

[18] N.L. Milic, S. Davis, J.M. Carr, S. Isberg, M.R. Beard, K.J. Helbig, Sequence analysis and characterisation of virally induced viperin in the saltwater crocodile (Crocodylus porosus), Dev. Comp. Immunol. 51 (2015) 108–115.

[19] B. Bushnell, J. Rood, E. Singer, BBMerge – accurate paired shotgun read merging via overlap, PLoS One 12 (2017) e0185056.

[20] A. Dobin, C.A. Davis, F. Schlesinger, J. Drenkow, C. Zaleski, S. Jha, P. Batut, M. Chaisson, T.R. Gingeras, STAR: ultrafast universal RNA-seq aligner, Bioinformatics 29 (2013) 15–21.

[21] A. Waardenberg, consensusDE: RNA-seq analysis using multiple algorithms, R package version 1 (22.0) (2024).

[22] M.I. Love, W. Huber, S. Anders, Moderated estimation of fold change and dispersion for RNA-seq data with DESeq2, Genome Biol. 15 (2014) 550.

[23] Y. Chen, L. Chen, A.T.L. Lun, P.L. Baldoni, G.K. Smyth, edgeR v4: powerful differential analysis of sequencing data with expanded functionality and improved support for small counts and larger datasets, Nucleic Acids Res. 53 (2025).

[24] M.E. Ritchie, B. Phipson, D. Wu, Y. Hu, C.W. Law, W. Shi, G.K. Smyth, Limma powers differential expression analyses for RNA-sequencing and microarray studies, Nucleic Acids Res. 43 (2015) e47.

[25] H. Wickham, ggplot2: Elegant Graphics for Data Analysis, Springer-Verlag, New York, 2016, ISBN 978-3-319-24277-4. https://ggplot2.tidyverse.org.

[26] G. Yu, L.G. Wang, Y. Han, Q.Y. He, clusterProfiler: an R package for comparing biological themes among gene clusters, OMICS 16 (2012) 284–287.

[27] G. Habarugira, J. Moran, J.J. Harrison, S.R. Isberg, J. Hobson-Peters, R.A. Hall, H. Bielefeldt-Ohmann, Evidence of infection with zoonotic mosquito-borne flaviviruses in saltwater crocodiles (Crocodylus porosus) in Northern Australia, Viruses 14 (2022).

[28] M. Merchant, M. Hebert, A.C. Salvador, J. Berken, T. Boverie, M.E. White, Constitutive innate immunity and systemic responses to infection of the American alligator (Alligator mississippiensis), Animals (Basel) 14 (2024).

[29] R. Siddiqui, A. Alvi, S. Alqassim, A.M. Alharbi, A. Alhazmi, N.A. Khan, Epigenetics and gut microbiome of reptiles can reveal potential targets to improve human health and performance, Discover Bacteria 2 (2025) 4.

[30] R. Siddiqui, N. Cruz Soares, N.A. Khan, Crocodile gut microbiome is a potential source of novel bioactive molecules, ACS Pharmacol. Transl. Sci. 4 (2021) 1260–1261.

[31] T.J. Chambers, M.S. Diamond, Pathogenesis of flavivirus encephalitis, Adv. Virus Res. 60 (2003) 273–342.

[32] R.N. Sempere, A. Arias, Establishment of a cell culture model of persistent flaviviral infection: Usutu virus shows sustained replication during passages and resistance to extinction by antiviral nucleosides, Viruses 11 (2019).

[33] H. Roth, V. Magg, F. Uch, P. Mutz, P. Klein, K. Haneke, V. Lohmann, R. Bartenschlager, O.T. Fackler, N. Locker, G. Stoecklin, A. Ruggieri, Flavivirus infection uncouples translation suppression from cellular stress responses, mBio 8 (2017).

[34] L. Mlera, W. Melik, M.E. Bloom, The role of viral persistence in flavivirus biology, Pathog Dis 71 (2014) 137–163.

[35] J. Herath, G. Ellepola, M. Meegaskumbura, Patterns of infection, origins, and transmission of ranaviruses among the ectothermic vertebrates of Asia, Ecol. Evol. 11 (2021) 15498–15519.

[36] Z. Zou, M. Li, Y. Zhou, J. Li, T. Pan, L. Lai, Q. Wang, L. Zhang, Q. Wang, Y. Song, Y. Zhang, Tumor necrosis Factor-α-Induced protein 8-Like 2 negatively regulates innate immunity against RNA virus by targeting RIG-I in macrophages, Front. Immunol. 12 (2021) 642715.

[37] M.Y. Zeng, I. Miralda, C.L. Armstrong, S.M. Uriarte, J. Bagaitkar, The roles of NADPH oxidase in modulating neutrophil effector responses, Mol Oral Microbiol 34 (2019) 27–38.

[38] S. van Wetering, N. van den Berk, J.D. van Buul, F.P. Mul, I. Lommerse, R. Mous, J. P. ten Klooster, J.J. Zwaginga, P.L. Hordijk, VCAM-1-mediated rac signaling controls endothelial cell-cell contacts and leukocyte transmigration, Am. J. Physiol. Cell Physiol. 285 (2003) C343–C352.

[39] Z. Wang, W. Li, S. Chen, X.X. Tang, Role of ADAM and ADAMTS proteases in pathological tissue remodeling, Cell Death Discov. 9 (2023) 447.

[40] S. Elmore, Apoptosis: a review of programmed cell death, Toxicol. Pathol. 35 (2007) 495–516.

[41] X. Zhu, Z. Chen, W. Shen, G. Huang, J.M. Sedivy, H. Wang, Z. Ju, Inflammation, epigenetics, and metabolism converge to cell senescence and ageing: the regulation and intervention, Signal Transduct. Targeted Ther. 6 (2021) 245.

[42] N.M. Elemam, I.M. Talaat, A.A. Maghazachi, CXCL10 chemokine: a critical player in RNA and DNA viral infections, Viruses 14 (2022).

[43] M.J. Trifilo, C. Montalto-Morrison, L.N. Stiles, K.R. Hurst, J.L. Hardison, J. E. Manning, P.S. Masters, T.E. Lane, CXC chemokine ligand 10 controls viral infection in the central nervous system: evidence for a role in innate immune response through recruitment and activation of natural killer cells, J. Virol. 78 (2004) 585–594.

[44] J. Han, Y. Yin, J. Yuan, Interplay between flaviviruses and the interferon response: mechanisms of immune evasion and therapeutic implications, Front. Pharmacol. 17 (2026) 1745652.

[45] J.L. Muñoz-Jordán, B.L. Fredericksen, How flaviviruses activate and suppress the interferon response, Viruses 2 (2010) 676–691.

[46] M.H. Orzalli, J.C. Kagan, Apoptosis and necroptosis as host defense strategies to prevent viral infection, Trends Cell Biol. 27 (2017) 800–809.